Sensorless Predictive Current Control of DC Motor

M. Seethamathavi
Student ME (PED),
Department of EEE,
Jay Shriram group of institutions,
Tiruppur, India

T. Vignesh
Associate Professor.
Department of EEE,
Jay Shriram group of institutions,
Tiruppur, India

***Abstract*-- For a sensor less predictive-peak-current-controlled boost converter, the output voltage steady-state error cannot be eliminated by voltage loop PI controller. The basic cause for this is investigated through analysis and theoretical approaches. To eliminate the voltage steady-state error and achieve high-accuracy current estimation, a comprehensive compensation strategy is proposed. First, a compensation algorithm for output voltage sampling is introduced. It can not only effectively eliminate the output voltage steady-state error but also guarantee current observer convergence. The compensation schemes for component parasitic parameter effects and switching delay are also investigated. With this comprehensive compensation strategy, both the system transient response and current estimation accuracy are greatly improved. Finally, the effectiveness of the proposed algorithm is verified by experimental results.**

Keywords: Differential current observer, MPPT, PMDC motor, PCC, Self-correction, Sensor less, SEPIC converter.

I. INTRODUCTION

In recent years, current control for a motor has become one of the research hot topics [1]-[6] compared with the voltage control mode, the current control mode has higher response speed and larger loop gain bandwidth. However, in current control mode, when the pulse width modulation (PWM) duty ratio is higher than 50%, a slope compensation circuit becomes necessary to maintain system stability. Due to its high robustness and high response speed, predictive current control (PCC) has been brought into sepic converter current control loop design and has been widely investigated. It has been extensively studied by many researchers [7-10].

In PCC mode, the inductor current of the next switching cycle should be predicted, and the duty ratio for the next switching cycle can be calculated according to the reference current and predicted current. Many PCC strategies have been proposed recently, but all the strategies need to sample the inductor current using a current sensor. Different current sensing techniques meet different applications in terms of cost, size, accuracy, isolation, *etc*. A thorough review of state-of-the-art current sensing techniques is presented in [11]. Sampling by a shunt resistor is found to be very simple, but is non-isolated and this causes high power losses. By using a complementary matching filter, sampling by the intrinsic resistance of the inductor brings no additional power losses and is very low-cost. However, the thermal drift is distinct and the accuracy could be low due to the mismatches between the filter and the power inductor [12, 13]. Fluxgate sensors have the highest performance at the cost of the highest price [11]. Rogowski coil sensors provide a wide measuring range and a high accuracy at relatively low cost [11]. Closed-loop AMR-based sensors have better performance than Hall-effect sensors, but smaller measuring range and higher cost. The GMI sensing system provides isolation with very low-cost [14, 15]. Nevertheless, the system requires frequent calibration due to its sensitivity to time and temperature..

The current sensors mentioned above all have different advantages and drawbacks, and thus could meet different requirements. However, existing techniques might not suit applications which require isolation with minimal price, power loss and size. Therefore, a current observer (CO) turns out to be a suitable substitute for conventional current sensors in digitally controlled converters. Current observers are used for motor controls, fault detection, and were firstly introduced for DC-DC applications by Midya [16]. The paper proposed an analog observation method for sensor less analog current mode control. However, the implementation does not suit digital controllers. For digitally controlled converters, an easy feed forward CO was proposed in 2004 [17].

In this application, the power converters transfer the Solar panel power to the load represented by a DC motor. As an advanced current control strategy, the predictive current control (PCC) has the characteristics of high robustness and high response speed. It can be combined with the current observer to realize sensor less PCC (SPCC). Both the PCC and current observer technologies have been widely investigated. For the PCC, an algorithm was investigated to eliminate the inductor current disturbance in one switching cycle in peak, average, and valley current control modes. However, in order to maintain the current control loop stability, the specific combination of current control mode with pulse width modulation (PWM) modulation scheme should be obeyed, and it restrains the flexibility of system design.

II. SENSORLESS PEAK CURRENT CONTROL

The construction of SEPIC DC-DC converter with the CO based PCC controller, is shown in Figure 1. The controller is a dual-loop system. The voltage loop is a PI compensator, which outputs the reference current I_{REF}. The current loop is the PCC controller, which calculates the duty ratio for the next switching cycle. In every switching cycle, the voltage sampling, the PI regulation, the current sensing and the PCC regulation are processed in sequence. In this way, the current error could be eliminated in two switching cycles.

Ignoring the parasitic parameters, a current differential equation can be derived based on the average voltage on the inductor, shown as equation 1,

$$LdIL(t)dt=DVIN(t)-VO(t) \quad (1)$$

where I_L, V_O, D, R and V_{IN} denote the inductor current, the output voltage, the duty ratio, the equivalent load resistor and the input voltage, respectively. The equation is the theoretical base for current observer.

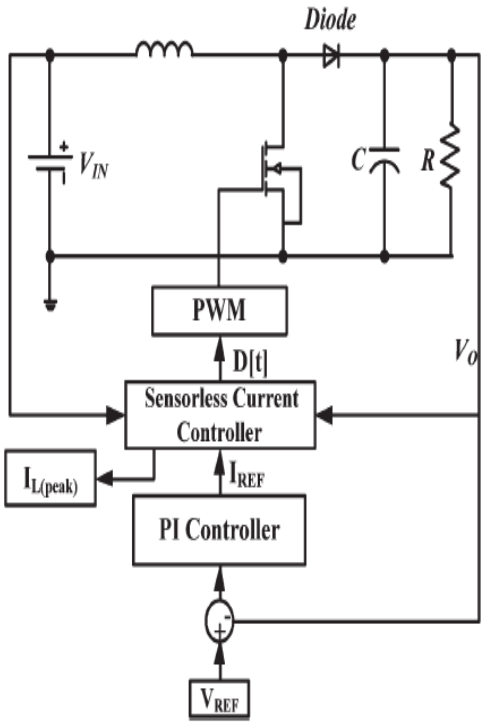

Fig 1. Structure of conventional sensorless current control for a boost converter.

A. Basic Current Observer

Based on equation 5, the inductor current can be observed using D, V_O, V_{IN}, L and T. In detail, for the kth switch cycle, the voltage absolute value on the inductor is $V_{IN}(k)-V_O(k)$ when the MOS switch is on, while being $V_O(k)$ when it is off. So, $M_1(k)$ and $M_2(k)$ can be written as equation 2

$$M1(k)=VIN(k)-VO(k)LM2(k)=VO(k)L \quad (2)$$

where $M_1(k)$ and $M_2(k)$ denote the positive slope and the negative slope of the inductor current, respectively. Meanwhile, the rising duration time of inductor current is $D(k)T$, and the falling duration time is $[1-D(k)]T$. Thus, the variation of the inductor current in the kth switching cycle can be written as equation 3

$$\hat{I}OB(k)=IOB(k+1)-IOB(k)=-M2(k)D'(k)T+M1(k)D \quad (k)T \quad (3)$$

where $I_{OB}(k)$ denotes the observed current, and $D'(k)$ is an abbreviation for $1-D(k)$. equation 3 is the basic current observer equation, from which the PCC algorithm is also derived.

B. Predictive Current Control

Employing valley current control and trailing edge (TE) modulation, the inductor current waveform is shown in Figure 2

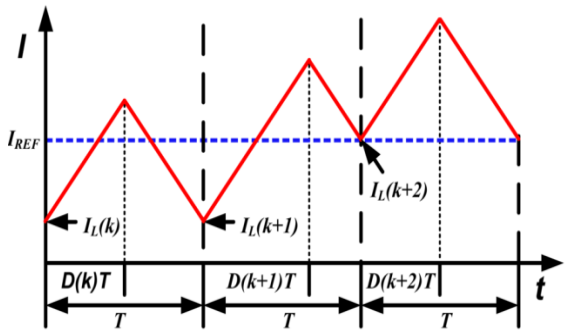

Fig 2 Current waveform under valley current control

I_{REF} is the reference current output from the PI regulator. There exists a deviation between $I_L(k)$ and I_{REF}. The PCC controller detects the current error, and adjusts the duty ratio $D(k+1)$, so that $I_L(k+2)$ reaches I_{REF}. In this way, the current error can be eliminated in two switching cycles.

As the switching cycle T is much shorter than the regulation time, the inductor current slope can be regarded as constant in two adjacent switching cycles, that is:

$$M1(k)=M1(k+1)=M1M2(k)=M2(k+1)=M2 \quad (4)$$

Substituting the control objective $I_{OB}(k+2) = I_{REF}$ equation 3, we have:

$$D(k+1)=IREF-IOB(k+1)+M2T(M1+M2)T \quad (5)$$

As shown above, the PCC controller can eliminate the current error in less than two switching cycles, which is relatively fast, so the converter can be designed with fast transient response. However, the CO-based PCC controller has problems such as the divergence of the observed current and the steady state error of the output voltage.

III. OUTPUT VOLTAGE STEADY-STATE ERROR ANALYSIS

For a current-mode-controlled boost converter with a current sensor, the voltage loop PI controller is able to eliminate ΔV_O, which is the steady-state error of the output voltage, by providing a pole at the origin. However, this conclusion does not necessarily apply for the SPCC because the pole at the origin from the PI controller's integration part is eliminated by the zero at the origin from SPCC. When there is no pole at the origin in the open-loop transfer function, the integration effect of the PI controller is nullified, and hence, the output voltage may have a steady-state error.

A. Basic Cause of ΔV_O

The closed-loop small-signal model in continuous time domain is shown in Fig. 3, where $G_{PI}(s)$, $G_{OB}(s)$, $T_{ID}(s)$, and $T_{DV}(s)$ are the transfer functions of the PI controller, I_{REF} to I_P , ΔI to duty ratio, and duty ratio to output voltage, respectively. Moreover, ΔI is equal to ($I_{REF} - I_P$). Assuming I_{REF} and I_P are sampled at the beginning of each switching cycle, then I_P strictly follows I_{REF} with two switching cycle delays.Transferring the above equation to continuous domain, then

$$I_L = \frac{1}{S_L}[V_{IN} - V_0(1-D)] \quad (6)$$

Impose small-signal disturbances $\hat{}I$REF, $\hat{}D$ and $\hat{}$ *VO* onto *I*REF, *D* and *VO*, respectively, and then substitute them into.

After eliminating dc elements and higher order infinitesimals, the following can be obtained:

$$\frac{\hat{I_L}}{\hat{D}} = \frac{1}{S_L}[V_O - \frac{\hat{V_O}}{\hat{D}}(1-D) \quad (7)$$

$G_{ID}(S)$is the transfer function from *D* to *IL*. Combining the self-correction module with the current observer, $G_{ID}(S)$is

$$G_{ID}(S) = \frac{\widehat{I_L}}{\hat{D}} = \frac{1}{(s+K)L}[V_O - \frac{\hat{V_O}}{\hat{D}}(1-D) \quad (8)$$

With regulating rule of PCC the G_{PCC} is derived. $G_{PCC}(s)$, i.e., the transfer function from ΔI to *D*, can be obtained by the same method, i.e.,

$$G_{PCC}(s) = \frac{L}{2T}\frac{1}{V_O - \frac{\hat{V_O}}{\hat{D}}(1-D)} \quad (9)$$

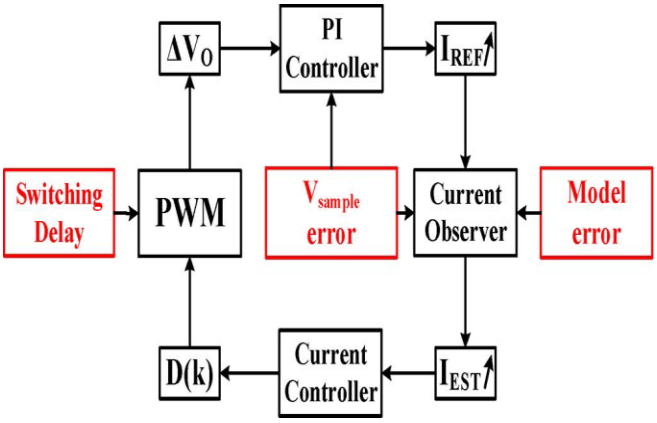

Fig 3. Generating process of the output voltage steady-state error.

B. Calculation of ΔV_O

Let I_P be the actual inductor peak current. When the system is in its steady state, the variation of I_P between the two neighbouring switching cycles is zero. In order to deduce $D(k + 1)$, it I only necessary to calculate ΔI rather than *IL*. After extracting common factor $1/sT$, ΔI becomes

$$\Delta I = I_{REF} - I_L = \frac{1}{sT}(\Delta I_{REF} - \Delta I_L) = \frac{1}{sT}\Delta I' \quad (10)$$

In , ΔIREF and ΔIL are the differential values of I_{REF} and *IL*, respectively. When the system reaches its steady state, both of them converge to zero, and the calculation overflow can be effectively avoided. ()

(6)

The current observer equation in the continuous domain can be converted , i.e.,

$$I_L = \frac{1}{sT}\frac{T}{L}[V_{IN} - V_O(1-D)] \quad (11)$$

Then the differential current observer is

(7)

$$\Delta I_L = \frac{T}{L}[V_{IN} - V_O(1\text{-}D)] \quad (12)$$

Whereas ΔIREF can be calculated by

$$\Delta I_{REF} = K_P(1 + 1/sT1)sT \quad (8) \quad (13)$$

Compared with the actual inductor current, the estimated inductor current has two switching cycle delays because of the digital control character. Hence, in the steady state, $\Delta I_{REF} = \Delta I_P$, ΔV_O can be obtained as

$$\Delta V_O = -[DT_1/(LK_P)]V_D \quad (14)$$

According to the above equations, ΔI_P and ΔV_O are proportional to V_D. In order to verify this conclusion, a simulation system of the boost converter was built under Simulink. The input voltage is 5 V, whereas the expected output voltage is 15 V. The main inductor is 28 μH, and V_D varies from 0 to 0.8V. The current loop control algorithm is based on (12), whereas the voltage loop is the PI controller.

The simulation results of different V_D versus ΔV_O fewer than two sets of PI controller parameters.

IV. EXPERIMENTAL RESULTS

To verify the proposed algorithm, experiments are carried out with a DC motor with sepic converter interface. SIMULINK model is created PMDC motor boost converter combination powered via a solar panel. This model contains renewable solar energy source, permanent magnet DC motor, and predictive current controller, control circuit which has PI controller, PWM. The waveforms based on these calculations are shown as follows.

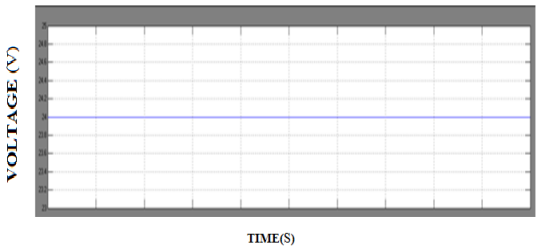

Fig 4. Input voltage

Fig 4 shows the input voltage of 24V, which is obtained from solar mppt. The MPPT algorithms are necessary in PV applications because the MPP of a solar panel varies with the irradiation and temperature, so the use of MPPT algorithms is required in order to obtain the maximum power from a solar array.

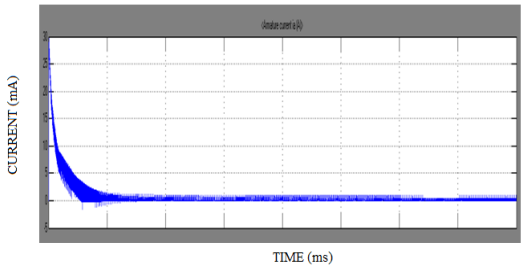

Fig 5. Armature current of the PMDC motor

Fig. 5 shows the output current obtained from simulation. On this basis, the system small-signal model, including the parasitic parameters, is constructed and analyzed. Then an SCDO is proposed. PMDC motor has high starting current and its getting reduced after the motor start to run at its desired speed.

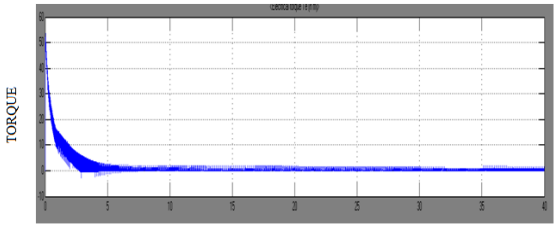

Fig 6. Torque of the PMDC motor

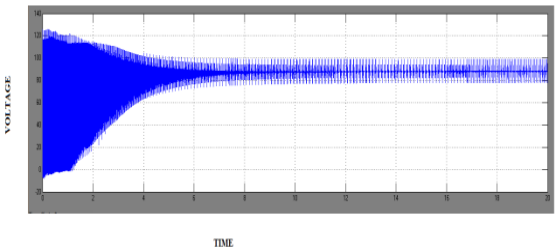

Fig 7. Output voltage of the PMDC motor

The basic cause of the output voltage steady-state error in a sensor less current-controlled sepic converter has been eliminated in fig 9 and it is proved through theoretical derivations.

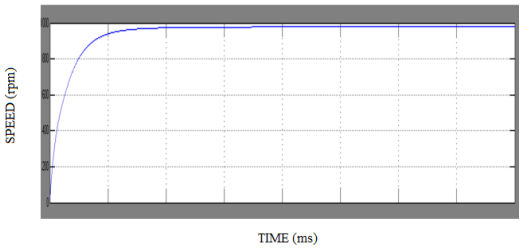

Fig 8. Speed of the PMDC motor

Fig 8 shows the speed of the motor and Fig 6 shows the torque of the motor. The above figures are matched with the practical performance of the PMDC motor. When the speed increases the torque and the armature current decreases. Speed is inversely proportional to the torque.

On this basis, the compensation strategy for output voltage sampling in both current loop and voltage loop has been proposed. In addition, the system modeling error caused by the parasitic parameters and nonlinear factors has been also compensated. The system ultimately achieves high-precision sensor less predictive peak current control without the voltage steady-state error with the comprehensive compensation strategy.

This boost converter could allow it to run on a large range of power with greater efficiency than simply reducing the voltage with a potentiometer to control the output. Most applications of the boost converter control the voltage automatically. Usually it is best to use the boost converter to hold a single output without the need for control when using a boost as part of a large circuit.

According to the preceding experimental results, even when the system is subject to sudden load and line voltage disturbances, it is able to respond quickly and converge to a new steady state with no output voltage steady-state error. With the proposed algorithm, the system shows good robustness.

V. CONCLUSION

The basic cause of the output voltage steady-state error in a sensor less current-controlled boost converter has been proved through theoretical derivations. On this basis,

the compensation strategy for output voltage sampling in both current loop and voltage loop has been proposed. In addition, the system modelling error caused by the parasitic parameters and nonlinear factors has been also compensated. The system ultimately achieves high-precision sensor less predictive peak current control without the voltage steady-state error with the comprehensive compensation strategy. Experimental results show that the control algorithm proposed in this paper is accurate and effective and has good potential for both theoretical and practical applications.

ACKNOWLEDGMENT

My sincere thanks to Dr.R.Maguteeswaran and Dr.P.Saravanan for their help and tremendous guidance without which the success of this project would not have been possible.

REFERENCES

[1] J. P. Wang, J. P. Xu, G. H. Zhou, and B. C. Bao, "Pulse-train-controlled CCM buck converter with small ESR output-capacitor," IEEE Trans. Ind. Electron., vol. 60, no. 12, pp. 5875–5881, Dec. 2013.

[2] M. Qin and J. P. Xu, "Improved pulse regulation control technique for switching dc–dc converters operating in DCM," IEEE Trans. Ind. Electron., vol. 60, no. 5, pp. 1819–1830, May 2013.

[3] Y. Yan, F. C. Lee, and P. Mattavelli, "Analysis and design of average current mode control using a describing-function-based equivalent circuit model," IEEE Trans. Power Electron., vol. 28, no. 10, pp. 4732–4741, Oct. 2013.

[4] J. A. A. Qahouq and V. P. Arikatla, "Power converter with digital sensorless adaptive voltage positioning control scheme," IEEE Trans. Ind.Electron., vol. 58, no. 9, pp. 4105–4116, Sep. 2011.

[5] J. Sha, J. Xu, B. Bao, and T. Yan, "Effects of circuit parameters on dynamics of current-mode-pulse-train-controlled buck converter," IEEE Trans. Ind. Electron., vol. 61, no. 3, pp. 1562–1573, Mar. 2014.

[6] V. Valdivia et al., "Black-box behavioral modeling and identification of dc–dc converters with input current control for fuel cell power conditioning," IEEE Trans. Ind. Electron., vol. 61, no. 4, pp. 1891–1903, Apr. 2014.

[7] Saggini, S.; Stefanutti, W.; Tedeschi, E.; Mattavelli, P. Digital deadbeat control tuning for DC-DC converters using error correlation. IEEE Trans Power Electron. 2007, 22, 1566–1570.

[8]Lai, Y.S.; Yeh, C.A. Predictive digital-controlled converter with peak current-mode control and leading-edge modulation. IEEE Trans Ind Electron. 2009.

[9]Bibian, S.; Jin, H. High performance predictive dead-beat digital controller for DC power supplies. IEEE Trans Power Electron. 2002. [10]Chen, J.; Prodic, A.; Erickson, R.; Maksimovic, D.Predictive digital current programmed control. IEEE Trans Power Electron. 2003.

[11] Ziegler, S.; Woodward, R.C.; Iu, H.; Borle, L.J. Current sensing techniques: A review. Sensors 2009.

[12]Dallago, E.; Passoni, M.; Sassone, G. Lossless current sensing in low-voltage high-current DC/DC modular supplies. IEEE Trans Ind Electron. 2000.

[13]Forghani-zadeh, H.P.; Rinco-Mora, G.A. An accurate, continuous, and lossless self-learning CMOS current-sensing scheme for inductor-based DC-DC converters. IEEE J Solid-State Circuits

[14]Jantaratana, P.; Sirisathitkul, C. Low-cost sensors based on the GMI effect in recycled transformer cores.Sensors 2008, 8, 1575–1584

[15]Ouyang, Y.; He, J.; Hu, J.; Wang, S.X. A current sensor based on the giant magnetoresistance effect: Design and potential smart grid applications. 2012

[16]P. Midya, P. T. Krein, and M. F. Greuel, "Sensorless current mode control—An observer-based technique for dc–dc converters," IEEE Trans.Power Electron., vol. 16, no. 4, pp. 522–526, Jul. 2001.

[17] P. Mattavelli, "Digital control of dc–dc boost converters with inductor current estimation," in Proc. 19th Annu. IEEE APEC, Feb. 2004, vol. 1,pp. 74–80.